Dynamic Behavior of Foundations

By Sakuro MURAYAMA and Kiichi TANIMOTO

Abstract

In this paper, studies on certain dynamic behavior concerning various kinds of foundation and a device of vibration measuring are reported in four separate sections.

The first section is a theoretical research on the consolidation settlement of a clayey ground, assuming the clay constitution to be a visco-elastic body constructed of an elastic element and a Voigt element in series. Though this assumption is adopted to solve the secondary time effect, sufficient experiments to examine this assumption are still left to the future. So this report can be described chiefly as a mathematical solution of the one-dimmensional consolidation of a clayey foundation due to such an oscillating load applied on the boundary as the periodical change of ground water pressure, machine vibration etc.

The second section is an experimental study on the gravel layer placed on the surface of the soft ground. The purpose of this study is to get some engineering information for designing such a gravel layer. One of the most important problems of the gravel layer lies in the railroad ballast bed, which is subjected to a heavy dynamic traffic load, especially in the case of the narrow gauge. The remarkable point which is cleared by this experiments is that the modulus of the ballast bed by the dynamic load varies with the vibration amplitude and differs from that by the static load.

The third section is a study on the free vibration of the foundation pile, which is an important element in earthquake-proof construction. In this section a newly devised method for numerical solution is introduced. With this method it is possible not only to calculate the eigenfrequency of the foundation pile subjected to any form of soil reaction pressure but also to solve general eigenvalue problems. Results by this method are checked with the rigorous solution and applied to the investigation of the field experiment of a reinforced concrete pile. In the experiment, the pile supports no vertical load, but the numerical solution may be developed to solve an actual foundation pile loaded with a heavy structure.

The fourth section is a report on an accelerometer made on trial to measure the low frequency vibration (5–50 c. p. s.) expected on the measurement in soil. This accelerometer is made with a small cantilever of a barium titanate ceramic bar as a vibration transducer, and has many merits such as good sensitivity, flat characteristics, small volume, same unit weight

with soils and cheap cost. After amplified, the excited piezoelectricity is recorded electro-optically by a galvanometer on bromide paper. With this accelerometer, the vibration displacement may be obtained by integrating the record of acceleration using a suitable integraph.

1. Consolidation Settlement of Clay Layer
Fundamental Equation

A rigorous mathematical solution of the process of consolidation of clay was already published by Terzaghi under the assumption that the constitution of the clay was an elastic body. This solution is not always correct for actual clays showing the so-called secondary time effect. To adapt the assumption to actual clay, the constitution of clay is assumed to be constructed of an elastic element and a Voigt element in series. In this section the consolidation settlement of the clay layer is solved mathematically not only for the static load but for such a dynamic load as the traffic load, the mechine vibration or the periodical change of ground water pressure. In the solution, the following assumptions are put forward; (a) The decrease of the volume of the voids of a fully saturated clay corresponds to the amount of water squeezed out. (b) For the consolidation by a dynamic load, the coefficient of swelling is equal to that of compression.

On the one-dimensional consolidation in z-direction, the total deformation, elastic one and final deformation of the Voigt element are designated by ε, ε_e and ε_v respectively, then

$$\varepsilon = \varepsilon_e + \varepsilon_v = (v_e + v_v)\, p\,, \qquad \cdots\cdots(1)$$

where p is the stress, and v_e and v_v the reciprocals of the spring constant of the elastic element and the Voigt element respectively.

For the Voigt model,

$$\frac{\partial \varepsilon_v}{\partial t} = -\eta(\varepsilon_v - v_v p)\,, \qquad \cdots\cdots(2)$$

where η is a coefficient of the model.

When p varies with time, the total deformation ε is given by

$$\varepsilon(z, t) = v_e p(z, t) + v_v \int_0^t \left[-\frac{\partial}{\partial t} \left\{ 1 - e^{-\eta(t-\tau)} \right\} \right] \cdot p(z, \tau)\, d\tau \qquad \cdots\cdots(3)$$

Differentiating Eq. (3),

$$\frac{\partial \varepsilon(x, t)}{\partial t} + \eta \varepsilon(z, t) - v_e \frac{\partial p(z, t)}{\partial t} + \eta(v_v - v_e)\, p(z, t) = 0 \qquad \cdots\cdots(4)$$

is obtained. From the assumption (a),

$$\frac{\partial \varepsilon(z, t)}{\partial t} = k \frac{\partial^2 w(z, t)}{\partial z^2}\,. \qquad \cdots\cdots(5)$$

where w is the pore-water pressure and k the coefficient of permeability. Elliminating ε and p from Eqs. (4), (5) and the relation $P(t)=p(z,t)+w(z,t)$, where $P(t)$ is the surcharged load, we get the following fundamental equation:

$$\frac{\partial^3 w}{\partial t \partial z^2}+\eta\frac{\partial^2 w}{\partial z^2}+\frac{v_e}{k}\frac{\partial^2 w}{\partial t^2}-\frac{\eta(v_p-v_e)}{k}\cdot\frac{\partial w}{\partial t} = \frac{v_e}{k}\frac{d^2P}{dt^2}-\frac{\eta(v_p-v_e)}{k}\cdot\frac{dP}{dt}. \qquad \cdots\cdots(6)$$

Solution of the Fundamental Equation for Dynamic Load

The fundamental equation (6) can be generally integrated, but it is solved for $v_e=0$ to calculate only the final deformation of the Voigt element. In this case, Eq. (6) is simplified as follows:

$$\frac{\partial^3 w(z,t)}{\partial t \partial z^2}+a\frac{\partial^2 w(z,t)}{\partial z^2}-b\frac{\partial w(z,t)}{\partial t}+b\frac{dP(t)}{dt}=0, \qquad \cdots\cdots(7)$$
$$a=\eta, \qquad b=\eta v_p/k.$$

Let us consider that a clay layer of thickness H is sandwiched between an impervious boundary at the surface and a pervious boundary at the bottom, and is stressed by a surface unit load $P(t)$. Hence, the initial and the boundary conditions are assumed as follows:

$$w(z,o)=P(0), \qquad \cdots\cdots(8)$$

$$\frac{\partial w(o,t)}{\partial z}=0, \qquad w(H,t)=0. \qquad \cdots\cdots(9)$$

The Laplace transform of Eq. (7) with respect to t is given by

$$\frac{\partial^2}{\partial z^2}\left\{su(z,s)-w(z,o)\right\}+a\frac{\partial^2 u(z,s)}{\partial z^2}-b\left\{su(z,s)-w(z,0)\right\} +b\left\{sh(s)-P(0)\right\}=0, \qquad \cdots(10)$$

where

$$u(z,s)=L_t\left\{w(z,t)\right\}=\int_0^\infty w(z,t)\,e^{-st}\,dt,$$
$$h(s)=L_t\left\{P(t)\right\}.$$

Substituting Eq. (8) into Eq. (10), we get

$$(s+a)\frac{\partial^2 u(z,s)}{\partial z^2}+bs\left\{h(s)-u(z,s)\right\}=0. \qquad \cdots\cdots(11)$$

The Laplace transform of Eq. (11) with respect to z is given by

$$(s+a)\left\{q^2\bar{u}(q,s)-qu(o,s)-\frac{\partial u(o,s)}{\partial z}\right\}+bs\left\{\frac{h(s)}{q}-\bar{u}(q,s)\right\}=0, \qquad \cdots(12)$$

where

$$\bar{u}(q, s) = L_z\left\{u(z, s)\right\} = \int_0^\infty u(z, s)\, e^{-qz}\, dz\,. \qquad \cdots\cdots(13)$$

Putting

$$\phi(s) = bs/(s+a) \qquad \cdots\cdots(14)$$

and applying the first equation of (9), to Eq. (13), we have

$$\bar{u}(q, s) = \frac{q}{q^2-\phi(s)}\, u(o, s) - \frac{\phi(s)}{q\{q^2-\phi(s)\}}\, h(s) \qquad \cdots\cdots(15)$$

By the inverse transformation with respect to z

$$u(z, s) = u(o, s)\cosh\sqrt{\phi(s)}\, z + h(s) \times (1-\cosh\sqrt{\phi(s)}\, z) \qquad \cdots(16)$$

is obtained and with the second equation of (9), Eq. (16) reduces to

$$u(z, s) = h(s)\left\{1-f(z, s)\right\}. \qquad \cdots\cdots(17)$$

where

$$f(z, s) = \cosh\sqrt{\phi(s)}\, z/\cosh\sqrt{\phi(s)}\, H\,. \qquad \cdots(18)$$

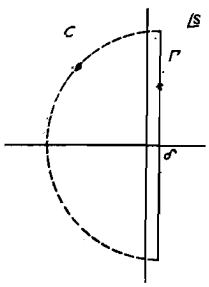

Fig. 1. Integration path cn complex plane s.

The inverse transformation of $f(z, s)$ is represented by an integral taken along a path on the complex plane of s as shown in Fig. 1. That is

$$F(z, t) = L_t^{-1}\left\{f(z, s)\right\} = \frac{1}{2\pi i}\lim_{\beta\to\infty}\int_{\delta-i\beta}^{\delta+i\beta} e^{st}\frac{\cosh\sqrt{\phi(s)}\, z}{\cosh\sqrt{\phi(s)}\, H}\, ds\,, \qquad \cdots(19)$$

where $\delta > 0$. When $F(z, t)$ is evaluated, $w(z, t)$ is proved to be

$$w(z, t) = P(t) - \int_0^t P(t-\tau)\, F(z, \tau)\, d\tau \qquad \cdots\cdots(20)$$

from Eq. (17). In Eq. (19) the integrand is analytic except for the zero points of the denominator. Then the integral $F(z, t)$ is equal to the summation of all residues of the poles existing in the domain whose boundaries are represented by Γ and C, because the integration along C vanishes when $\beta \to \infty$. The values of s which make the denominator of the integrand zero are

$$s_n = \frac{-a\beta_n^2}{b+\beta_n^2}, \qquad \beta_n = \frac{2n+1}{2H}\pi (n = 0, 1, 2, \cdots)\,, \qquad \cdots\cdots(21)$$

and s_n is negative, as a and b are both positive.

The residue ρ_n at the pole $s = s_n$ is

$$\rho_n = 2(-1)^n \frac{ab\beta_n}{H(b+\beta_n^2)^2}\cos\beta_n z \cdot e^{s_n t}\,, \qquad \cdots\cdots(22)$$

Then

$$F(z, t) = \sum_{n=0}^{\infty} \rho_n = \frac{2ab}{H} \sum_{n=0}^{\infty} (-1)^n (s_n + a)^2 \beta_n \cos \beta_n z \cdot e^{s_n t} \quad \cdots(23)$$

Substituting this into Eq. (20), we get the solution $w(z, t)$ as

$$w(z, t) = P(t) - \frac{2ab}{H} \sum_{n=0}^{\infty} (-1)^n \frac{\beta_n}{(b + \beta_n^2)^2} \cos \beta_n z \int_0^t P(t-\tau)\, e^{s_n t}\, d\tau \cdots(24)$$

Further Investigation on the Above Solution

We shall investigate Eq. (24) for some special cases.

(A) when $\eta = \infty$, $P(t) = P_0$ (const)

$$w(z, t) = 2P_0 \sum_{n=0}^{\infty} (-1)^n \frac{\cos \beta_n z}{\beta_n H} e^{-\frac{k}{v_p} \beta_n^2 t} \quad \cdots\cdots\cdots\cdots(25)$$

This is the same result as Terzaghi's.

(B) when $P(t) = P_0 \cos \omega t$, ω: circular frequency

In practice, tensile stress cannot occur in soil, so that we must add the static load which cancels at least the negative vibrating load. Disregarding the influence of the added static load, however, we shall deal exclusively with only the vibrating load in this case, then the equation of the pore-water pressure by only the vibrating load takes the form:

$$w(z, t) = P_0 \cos \omega t - \frac{2abP_0}{H} \sum_{n=0}^{\infty} (-1)^n \frac{\beta_n \cos \beta_n z}{(b + \beta_n^2)^2 (\omega^2 + s_n^2)} \times \left\{ -s_n (\cos \omega t - e^{s_n t}) - \omega \sin \omega t \right\} \quad \cdots\cdots(26)$$

As the successive terms decrease with the order β_n^{-3}, it is sufficient to approximate Eq. (26) by its first term as follows:

$$w(z, t) \simeq P_0 \cos \omega t - \frac{4abH^2 P_0 \pi \cos \frac{\pi z}{2H}}{\omega^2 (4bH^2 + \pi^2)^2 + a^2 \pi^4} \times \left\{ a\pi^2 (\cos \omega t - e^{-\frac{a\pi^2}{4bH^2 + \pi^2} t}) - \omega \sin \omega t (4bH^2 + \pi^2) \right\}. \quad \cdots(27)$$

Since the pore-water pressure varies with t in Eq. (27), the direction of the seepage flow cannot be constant. It is only the exponential term in Eq. (27) that influences the seepage flow in one cycle of the oscillation, and this term is denoted $\bar{w}(z, t)$.

$$\bar{w}(z, t) = \frac{4a^2 bH^2 P_0 \pi^3}{\omega^2 (4bH^2 + \pi^2)^2 + a^2 \pi^4} \cos \frac{\pi z}{2H} \cdot e^{-\frac{a\pi^2}{4bH^2 + \pi^2} t} \quad \cdots\cdots(28)$$

Denoting the quantity of water squeezed out of the clay layer by Q, we have

$$Q = k\int_0^t \frac{\partial^2 \bar{w}}{\partial z^2}\,dt = \bar{c}\cos\frac{\pi z}{2H}\,(e^{-\xi t}-1) \qquad \cdots\cdots(29)$$

where

$$\bar{c} = \frac{ab\pi^3(4bH^2+\pi^2)\,P_0 k}{\omega^2(4bH^2+\pi^2)^2+a^2\pi^4}, \qquad \xi = \frac{a\pi^2}{4bH^2+\pi^2}. \qquad \cdots\cdots(30)$$

According to Eq. (29), Q has a certain limit. The value ξ varies with a, b and H, and is large when the elastic property of the Voigt element is superior to the plastic one and vice versa. If $\xi \simeq 1$, we can easily derive the conclusions in two cases for ω.

i) when $\omega \gg 1$, $\xi \simeq 1$
From Eq. (27)

$$w(z,t) = P_0\cos\omega t + \frac{4abH^2\pi P_0}{\omega(4bH^2+\pi^2)}\cos\frac{\pi z}{2H}\sin\omega t, \qquad \cdots\cdots(31)$$

and as the second term is negligibly small compared with the first term on the right hand side, $w(z,t)$ is nearly equal to the external load and does not damp with time.

ii) when $\omega \ll 1$, $\xi \simeq 1$

$$w(z,t) = P_0\left(1-\frac{4bH^2}{\pi}\cos\frac{\pi z}{2H}\right)\cos\omega t + \frac{4bH^2P_0}{\pi}\cos\frac{\pi z}{2H}\cdot e^{-\frac{a\pi^2}{4bH^2+\pi^2}t} \qquad \cdots(32)$$

Here the effect of the damping term is left until t becomes very large, and the amplitude of the harmonic term is governed by viscosity.

(C) when $P(t) = \begin{cases} P_0 \text{ (const)} & \text{for } T>t>0 \\ 0 & \text{for } t>T \end{cases}$

This is the case of the impact work from $t=0$ till $t=T$ and if $s_0 T \ll 1$, for $T>t>0$

$$w(z,t) \simeq P(t) + \frac{2bs_0P_0t}{H\beta_0(b+\beta_0^2)}\cos\beta_0 z. \qquad \cdots\cdots(33)$$

For $t>T$

$$w(z,t) \simeq \frac{2bs_0P_0T}{H\beta_0(b+\beta_0^2)}\cos\beta_0 z\cdot e^{s_0 t} \qquad \cdots\cdots(34)$$

The pore-water pressure damps with the relaxation time:

$$-\frac{1}{s_0} = \frac{a\pi^2}{4bH^2+\pi^2}. \qquad \cdots\cdots(35)$$

Solution for a static Load—as a Case of the Consolidation Test

Since $P(t) = \text{const}$ $(\equiv P)$ in this case, the fundamental equation (6) reduces to

$$\frac{\partial^3 w}{\partial t\partial z^2} + \eta\frac{\partial^2 w}{\partial z^2} + \frac{v_e}{k}\frac{\partial^2 w}{\partial t^2} - \frac{\eta(v_p-v_e)}{k}\frac{\partial w}{\partial t} = 0. \qquad \cdots\cdots(36)$$

The initial and the boundary conditions are assumed as follows:

$$w(z, o) = P$$
$$w(o, t) = 0, \quad w(H, t) = 0. \qquad \cdots\cdots(37)$$

Applying the Laplace transformation, the solution of Eq. (37) is given by

$$w(z, t) = \frac{4P}{\pi} \sum_{n=1,3,5\cdots}^{\infty} \frac{1}{n} (Ae^{\lambda_1 t} + Be^{\lambda_2 t}) \sin \frac{n\pi z}{H} \qquad \cdots\cdots(38)$$

where

$$\left.\begin{matrix}\lambda_1 \\ \lambda_2\end{matrix}\right\} = \frac{1}{2v_e}\left[-(v_e+v_p)\,\eta - k\left(\frac{n\pi}{H}\right)^2 \pm \sqrt{\left\{(v_e+v_p)\,\eta + k\left(\frac{n\pi}{H}\right)^2\right\}^2 - 4v_e\eta k\left(\frac{n\pi}{H}\right)^2}\right]$$

$$A = -k\left(\frac{n\pi}{H}\right)^2 \cdot \frac{(\lambda_1+\eta)^2}{\lambda_1\{v_e(\lambda_1+\eta)^2 + \eta^2 v_p\}} \qquad \cdots\cdots(39)$$

$$B = -k\left(\frac{n\pi}{H}\right)^2 \cdot \frac{(\lambda_2+\eta)^2}{\lambda_2\{v_e(\lambda_2+\eta)^2 + \eta^2 v_p\}}$$

Then the degree of consolidation μ is calculated as follows:

$$\mu = 1 - \frac{8}{\pi^2}\frac{v_e}{v_e+v_p} \sum_{n=1,3,5\cdots}^{\infty} \frac{1}{n^2} (Ae^{\lambda_1 t} + Be^{\lambda_2 t}) - \frac{8}{\pi^2}\frac{v_p}{v_e+v_p} \qquad \cdots\cdots(40)$$
$$\sum_{n=1,3,5}^{\infty} \frac{1}{n^2}\left(\frac{\eta A}{\lambda_1+\eta} e^{\lambda_1 t} + \frac{\eta B}{\lambda_2+\eta} e^{\lambda_2 t}\right).$$

Putting

$$\frac{k}{v}\left(\frac{n\pi}{H}\right)^2 \Big/ \eta = x, \qquad \frac{\gamma}{v} = c, \qquad \cdots\cdots(41)$$

we get

$$\lambda_1 = -\eta\left\{(1+c+x) - \frac{x}{1+c+x} - \frac{x^2}{(1+c+x)^2} - \cdots\right\}, \qquad \cdots\cdots(42)$$

and

$$\lambda_2 = -\eta\left\{\frac{x}{1+c+x} + \frac{x^2}{(1+c+x)^2} + \cdots\right\}. \qquad \cdots\cdots(43)$$

In the following two cases, we investigate Eq. (40).

i) when $x \ll 1$

As $\lambda_1 \simeq -\eta(1+c)$, $\lambda_2 \simeq -\frac{1}{1+c}\cdot\frac{k}{v_e}\left(\frac{n\pi}{H}\right)^2$, $A \simeq 0$, $B \simeq 1$, $\frac{\eta A}{\lambda_1+\eta} \simeq 0$ and $\frac{\eta B}{\lambda_2+\eta} \simeq 1$, μ is given by

$$\mu \simeq 1 - \frac{8}{\pi^2} \sum_{n=1,3,5\cdots}^{\infty} \frac{1}{n^2} e^{-\frac{k}{v_e+v_p}\left(\frac{n\pi}{H}\right)^2 t} \qquad \cdots\cdots(44)$$

ii) when $x \gg 1$

As $\lambda_1 \simeq -\frac{k}{v_e}\left(\frac{n\pi}{H}\right)^2$, $\lambda_2 \simeq -\eta$, $A \simeq 1$, $B \simeq 0$, $\frac{\eta A}{\lambda_1+\eta} \simeq 0$ and $\frac{\eta B}{\lambda_2+\eta} \simeq 1$, μ is given by

$$\mu \simeq 1 - \frac{8}{\pi^2}\frac{v_e}{v_e+v_p} \sum_{n=1,3,5\cdots}^{\infty} \frac{1}{n^2} e^{-\frac{k}{v_e}\left(\frac{n\pi}{H}\right)^2} - \frac{8}{\pi^2}\frac{v_p}{v_e+v_p} \sum_{n=1,3,5\cdots}^{\infty} \frac{1}{n^2} e^{-\eta t} \qquad (45)$$

The obtained $\mu - \log t$ curves for various values of x and c are shown in Figs. 2~5.

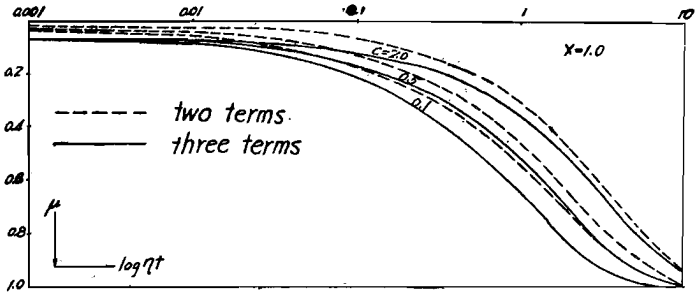

Fig. 2

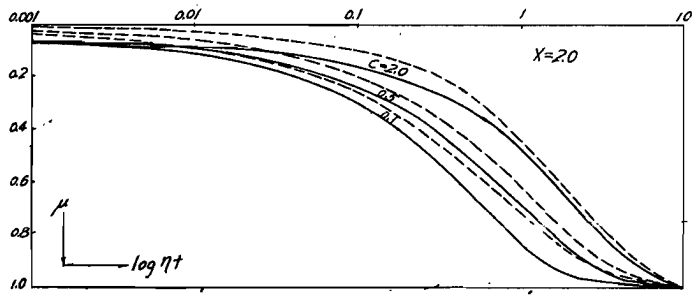

Fig. 3

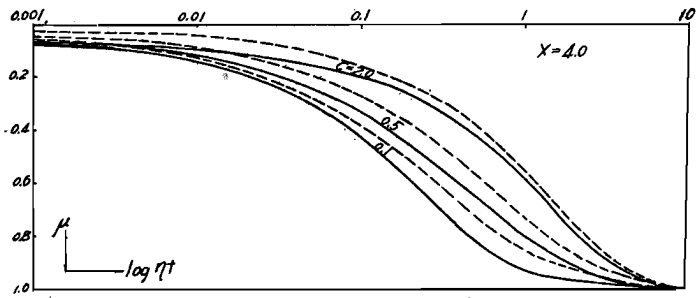

Fig. 4

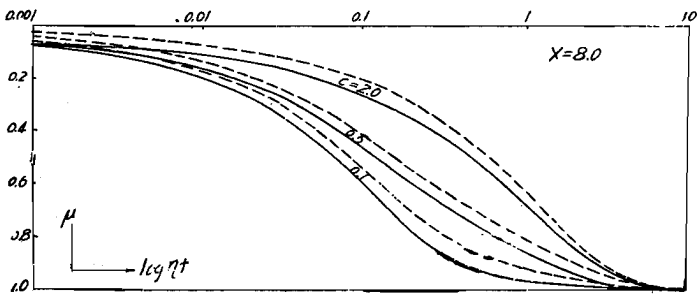

Fig. 5

Fig. 2~5. Theoretical $\mu - \log t$ curves for $x=1.0$, 2.0, 4.0, 8.0 and $C=0.1$, 0.5, 2.0.

2. Experimental Studies on Gravel Beds under Dynamic Loads

Model Experiments

The most typical example of the gravel bed is the railroad ballast. Besides this, gravel or sandy gravel beds are frequently found in the underlying layer of such various structures built on soft ground as pavements or footings. This article is a report about vibrational characteristics of the gravel bed studied experimentally with small models.

Vibration is produced by a two-mass oscillator driven by 1/50 HP. A. C. motor. The oscillator weighs 3.93 kg and has a base of 135 mm × 160 mm dimensions. As its eccentric masses the following four kinds are used: A : 2.6 gr, B : 19.7 gr, C : 26.55 gr, D : 37.43 gr.

The model gravel beds are made of gravels as shown in Table 1 for every thickness of the beds, and are surrounded by U-shaped wooden frames on three sides and are placed on sponge rubber of 52 cm × 53 cm wide and 1 cm thick simulating soft ground. Every side of the wooden frames is 30 cm or 50 cm in length, and cotton 6 mm thick is inserted between the inner sides of the frames and the graval to remove the effect of reflective waves from the frames.

Table 1. Model gravel beds used in exeriment

side length of frame 50 cm		side length of frame 30 cm	
thickness of layer	size of grain	thickness of layer	size of grain
5 cm	0~5 mm	5 cm	0~5mm
10	5~10	10	5~10
15	10~15	15	10~15

In this experiment, the frequency of the oscillator is controlled in the range of 0~50 c. p. s., and the vibration displacement is measured optically at the center of the base of the oscillator.

The displacement amplitude-frequency curves obtained are shown in Figs. 6~11, where t is thickness of the bed, s grain size and f side length of the frame. These figures show the relations corrected to correspond to a constant oscillating force for each case from the actually measured relations, with the consideration that the actual oscillating force increases in proportion to the square of frequency. It is seen that the resonance frequency appears in the neighbourhoods of 10 c. p. s. and 35 c. p. s. and peaks change with the oscillating force, showing the nonlinear vibrational characteristics.

An Approximate Determination of Restoring Characteristics

In order to determine restoring characteristics of the model gravel bed, such a simple vibration system is assumed as to be given by the following equation ;

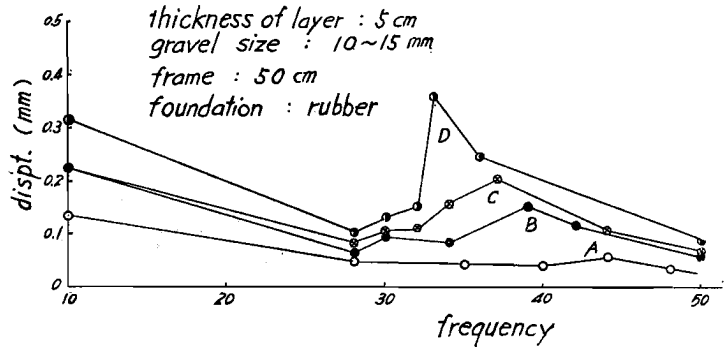

Fig. 6

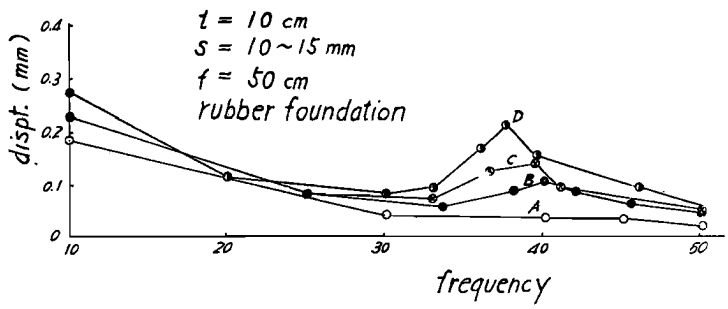

Fig 7

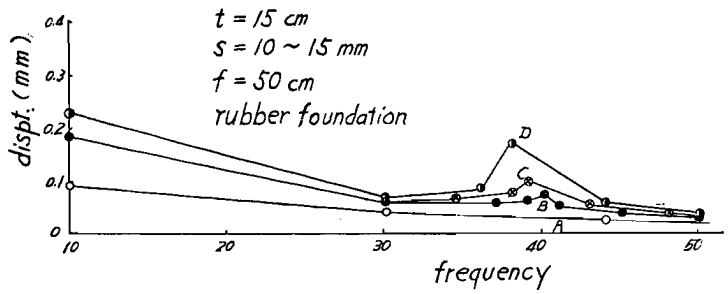

Fig. 8

Fig. 6~8. Displacement amplitude-frequency curves of model gravel bed for various kinds of thickness, grain size and side length of frame.

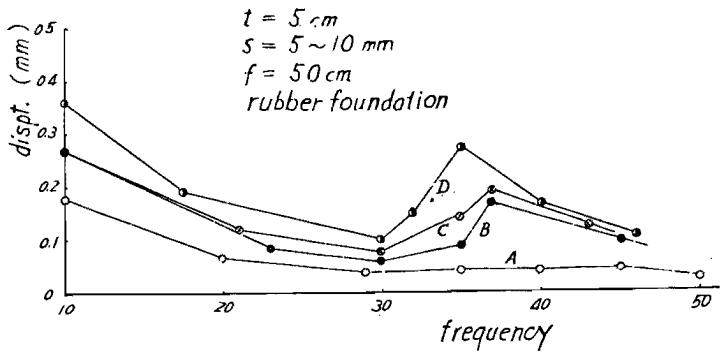

Fig. 9

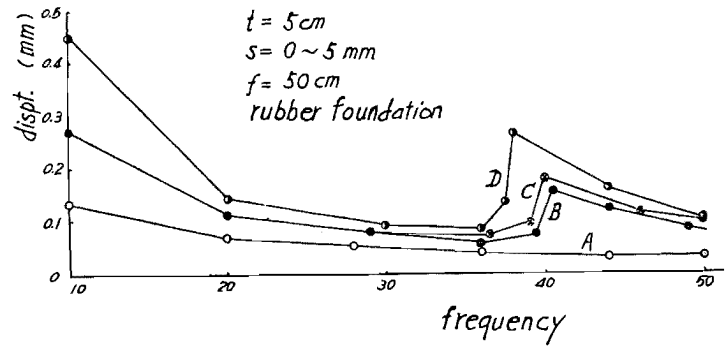

Fig. 10

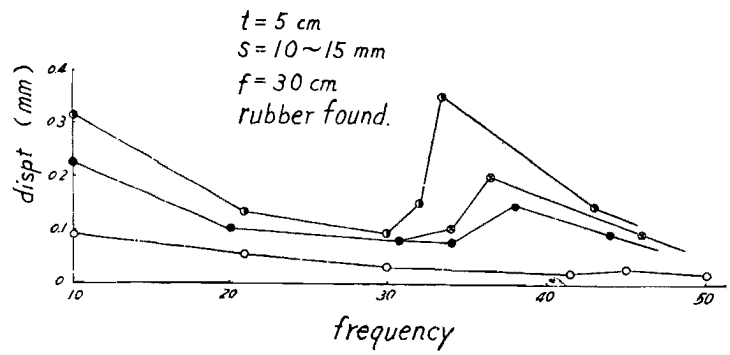

Fig. 11

Fig. 9~11. Displacement amplitude-frequency curves of model gravel bed for various kinds of thickness, grain size and side length of frame.

$$M\frac{d^2x}{dt^2}+f(x)=P\cos\omega t\,, \qquad \cdots\cdots(46)$$

where

M: equivalent mass, that is the summ of mass of the oscillator and effective virtual mass of foundation per unit area of the base plate of the oscillator

x: vertical displacement of the base plate

$f(x)$: restoring force of the foundation per unit area of the base plate

P: oscillating force per unit area of the base plate

ω: circular frequency of oscillation.

According to the D. Hartog's method,[1)]

$$x=a\cos\omega t \qquad \cdots\cdots(47)$$

is assumed, then the maximum value of the inertia force is given by $Ma\omega^2$, and if both the oscillating force and the restoring force become their maximum values when the inertia force is its maximum, we get

$$f(a)=Ma\omega^2+P=Ma\omega^2+mr\omega^2\,, \qquad \cdots\cdots(48)$$

where m and r denote the eccentric mass and its eccentric radius respectively. As no reliable and practicable methods have been developed which would permit the numerical determination of M, it is assumed that the equivalent mass M is given by the following equation,

$$M=\frac{1}{aF}(\overline{M}_1a+\overline{M}_2a_2+\overline{M}_3a_3) \qquad \cdots\cdots(49)$$

where

F: area of base plate of the osicillator

$\overline{M}_1$: mass of oscillator

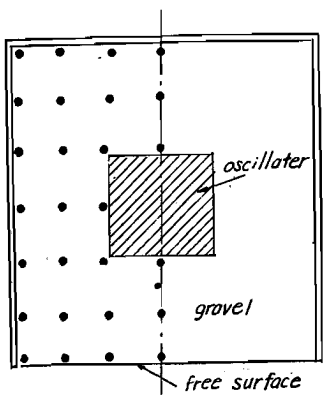

Fig. 12. Location of measuring points to determine a_2 and a_3.

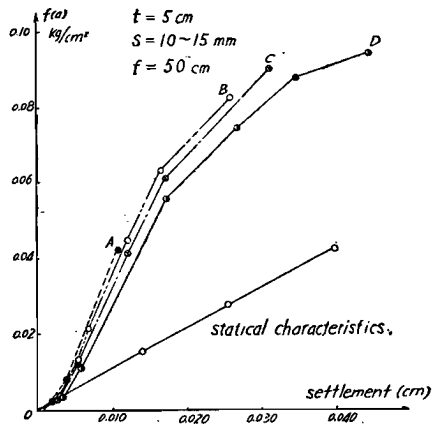

Fig. 13. Restoring characteristics of model gravel bed.

$\overline{M}_2$: mass of whole vibrating gravel layer
$\overline{M}_3$: mass of whole vibrating sponge rubber
a_2: average value of vibration displacement of gravel layer
a_3: average value of vibration displacement of sponge rubber

The approximate values of a_2 and a_3 are obtained by measuring the vibration amplitudes of the embedded small wooden rods in each material, whose locations are shown in Fig. 12. The restoring forces obtained by substitution of these values into Eq. (48) are given in Figs. 13~15. In these figures, static characteristics are added to compare with dynamic ones.

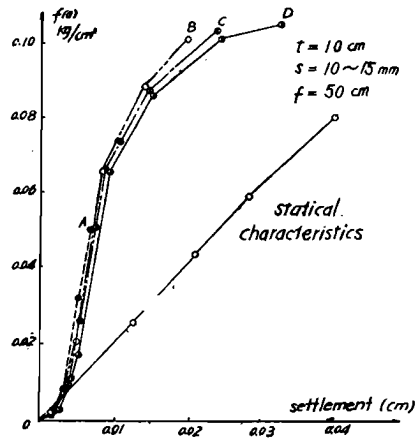

Fig. 14. Restoring characteristics of model gravel bed.

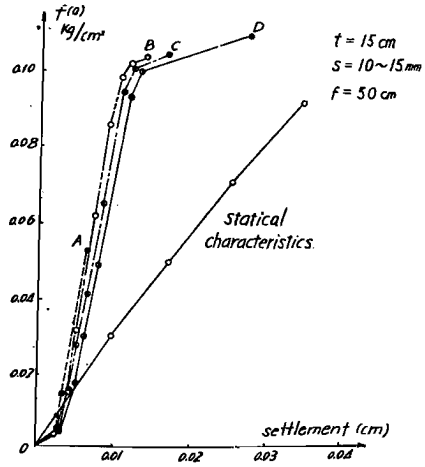

Fig. 15. Restoring characteristics of model gravel bed.

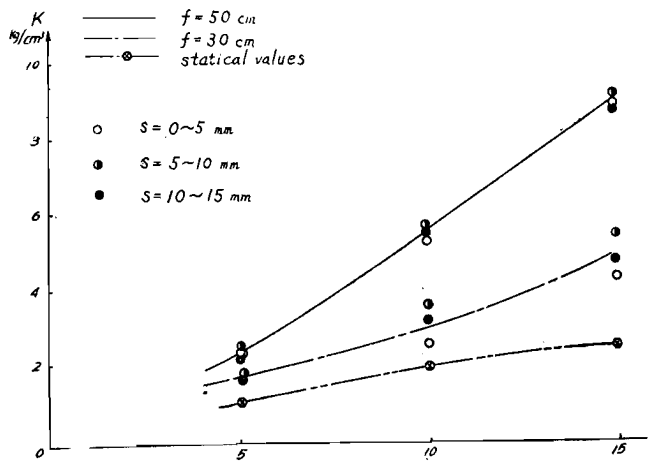

Fig. 16. Dependency of dynamic modulus K of gravel bed on dimensions of bed and grain size s.

The modulus of the gravel bed (K) is expressed by the first derivative of $f(x)$, that is, the inclination of the tangent line on each curve in Figs. 13~15, so it can be seen that the dynamical modulus of the gravel bed varies with various factors. The modulus K for $\omega = 2\pi \times 35$ c.p.s. relating to the thickness and the area of the gravel layer and the grain size is obtained with the model experiments as shown in Fig. 16.

Experiments with Full-size Rail road Ballast Bed

The test track is made of river ballast (size 15 mm~65 mm) 15 cm thick, placed on soft silty clay with sleepers 70 cm apart and 37 kg-rails 10 m long in narrow gauge (1067 mm) as shown in Fig. 17.

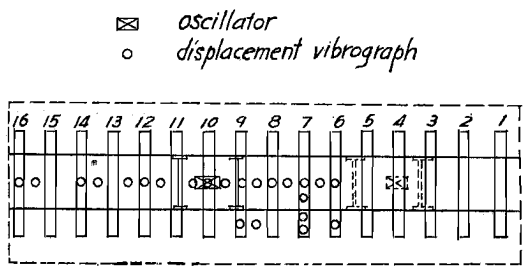

Fig. 17. Plan of the test trank and the arrangement of measuring apparatus.

This track is vibrated by a two-mass oscillator fixed on a trolly on the rails. The oscillator weighs about 100 kg and is driven by a variable speed motor of 1/2 HP., and can generate about 600 kg of oscillating force at 25 c.p.s. by twelve detachable eccentric masses weighing 0.16 kg each.

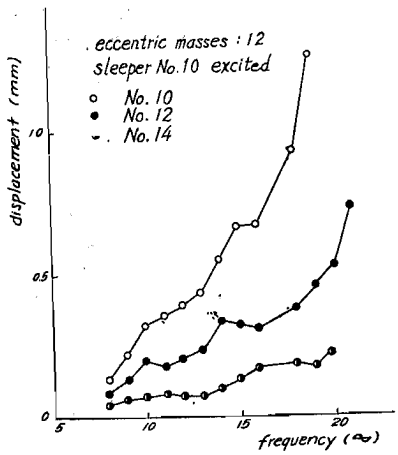

Fig. 18. Relations between vibration displacement of sleeper and frequency of oscillator.

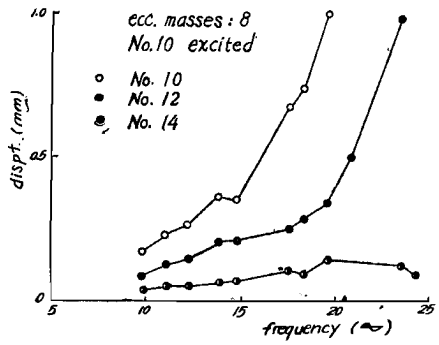

Fig. 19. Relations between vibration displacement of sleeper and frequency of oscillator.

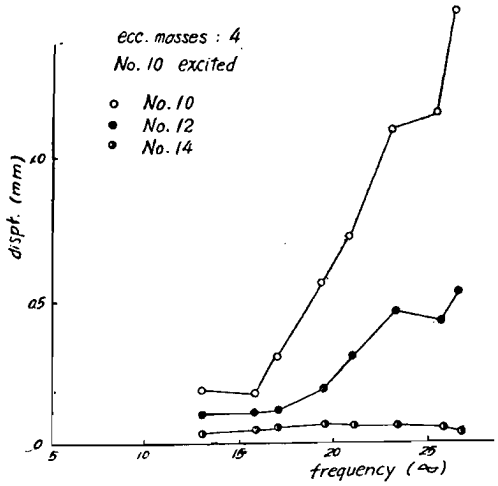

Fig. 20. Relations between vibration displacement of sleeper and frequency of oscillator.

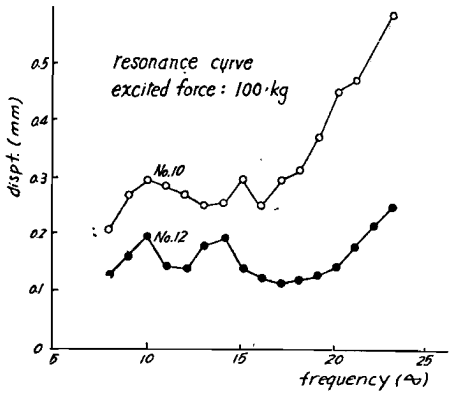

Fig. 21. Resonance curves of sleeper.

Measuring the vibration displacement of the ballast and the sleepers with moving-coil-type vibration pick-ups and an electro-optical recorder, the relations of the vibration displacement of the sleepers to the frequency of the oscillator are obtained as shown in Figs. 18, 19 and 20, and the resonance curve is given by Fig. 21. In Fig. 21, a peak of the curve appears at about 10 c. p. s., but it is somewhat questionable to conclude this to be a resonance point since the peak is so low. But the next peak cannot be caught until about 25 c. p. s. which is the limit of the oscillator used.

According to the results of the measurement on the ballast, the vibration displacement of the ballast surface has a tendency similar to that of the

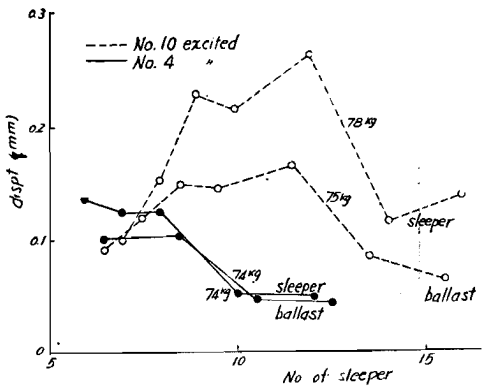

Fig. 22. Longitudinal distribution of vibration displacement of sleepers and ballast.

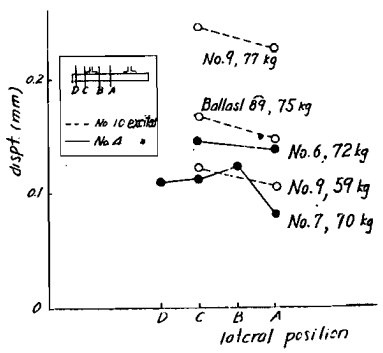

Fig. 23. Lateral distribution of vibration displacement of sleepers and ballast.

sleeper, but is somewhat smaller. Figs. 22 and 23 show the distribution of the vibration displacement of both ballast and sleepers in the longitudinal and lateral directions of the track when the trolly is placed on the sleepers Nos. 9–11 (dotted lines) and Nos. 3–5 (full lines). From Fig. 23 it is seen that the sleeper jumps vertically, vibrating in the vertical plane, and the amplitude of its vibration seems to be extremely smaller than the amount of the jump. The reason why the transverse distribution of the vibration of the ballast is almost uniform seems to be due to this fact.

3. Free Transverse Vibration of Foundation Pile

Fundamental Equation of Transverse Vibration

In this section, the eigenfrequency of the foundation pile driven in the ground is researched. The fundamental differential equation of the transverse vibration of the vertical pile subjected to the horizontal load $f(x, t)$ is given by

$$EI\frac{\partial^4 y}{\partial x^4}+\frac{\rho A}{g}\cdot\frac{\partial^2 y}{\partial t^2}+yK(x)=f(x, t)\,, \qquad \cdots\cdots\cdots\cdots(50)$$

where x is a coodinate selected vertically downward from the center of the pile head, and y the horizontal deflection from x-axis, EI, ρ and A are the flexural rigidity, unit weight and the sectional area of the pile, and $K(x)$ the reaction force by the ground along the unit length of the pile.

On the free vibration, neglecting the term of the right hand side, Eq. (50) becomes

$$EI\frac{\partial^4 y}{\partial x^4}+\frac{\rho A}{g}\frac{\partial^2 y}{\partial t^2}+yK(x)=0\,. \qquad \cdots\cdots\cdots\cdots(51)$$

If the distribution of the earth pressure reaction $K(x)$, has complex form, the solution of Eq. (51) is hardly integrated analytically. To overcome such a difficult case, we try to calculate numerically by the following method newly divised.

A Numerical Solution of Eigenfrequency Equation

In order to solve eigenfrequency equations which are difficult or impossible to solve analytically, the authors have devised a numerical solution. This method is an extension of the Kimball and Shortley's method[2] in quantum mechanics, and may be applied not only to the free vibration of an elastic body but also to general eigenvalue problems. Here we explain some general cases.

A) Eigenfrequency problem of the second order

Suppose the fundamental equation of the free vibration of a string:

$$\frac{\partial^2 y(x, t)}{\partial t^2}=c^2\frac{\partial^2 y(x, t)}{\partial x^2} \qquad (0\leqq x\leqq l)\,, \qquad \cdots\cdots\cdots\cdots(52)$$

where c is a constant. By the suitable transformation of x and t, Eq. (52) becomes

$$\frac{\partial^2 y(x,t)}{\partial t^2} = \frac{\partial^2 y(x,t)}{\partial x^2} \qquad (0 \leqq x \leqq 1). \qquad \cdots\cdots(53)$$

Substituting $y(x,t) = \bar{y}(x)e^{ipt}$ into Eq. (53), we get

$$\frac{d^2\bar{y}(x)}{dx^2} + \lambda\bar{y}(x) = 0, \quad \lambda = p^2. \qquad \cdots\cdots(54)$$

If there exists non-vanishing $\bar{y}(x)$ under certain boundary conditions, $\bar{y}(x)$ is called the eigenfunction and λ the corresponding eigenvalue. Hereafter $y(x)$ is used instead of $\bar{y}(x)$.

In order to integrate numerically Eq. (54), this equation is approximately replaced by the difference equation. The domain $0 \leqq x \leqq 1$ is divided into N equal parts, and the divided points are denoted by x_i $(i = 1, 2, \ldots, N-1)$ and the extreme points by x_0 and x_N $(x_0 = 0, x_N = 1)$. If x is an arbitrary value which satisfies $x_0 < x < x_1$, the value of the corresponding y is given by Stirling's interporation formula as follows:

$$y = y_0 + \frac{u}{1!}\cdot\frac{\Delta y_{-1} + \Delta y_0}{2} + \frac{u^2}{2!}\Delta^2 y_{-1} + \frac{u(u^2-1)}{3!}\cdot\frac{\Delta^3 y_{-2} + \Delta^3 y_{-1}}{2} + \cdots \qquad \cdots(55)$$

where $u = \dfrac{x-x_0}{x_1-x_0} = \dfrac{x-x_0}{\Delta x}$. Differentiating Eq. (55) twice, we have the following equation as the first approximation.

$$\left(\frac{d^2y}{dx^2}\right)_{x=x_0} \simeq \frac{1}{(\Delta x)^2}(y_1 - 2y_0 + y_{-1}). \qquad \cdots\cdots(56)$$

For every divided point x_k, Eq. (54) is replaced approximately by the algebraic equation:

$$\lambda y_k = \frac{-y_{k+1} + 2y_k - y_{k-1}}{(\Delta x)^2}. \qquad \cdots\cdots(57)$$

Here Eq. (57) is generally rewritten as the summation form:

$$(\Delta x)^2 \lambda y_k = \sum_{i=0}^{N} b_{ki} y_i. \qquad \cdots\cdots(58)$$

The coefficient b_{ki} in Eq. (58) is the element of the following matrix (b_{ki}), which can be expressed as the form:

$$(b_{ki}) = \begin{pmatrix} 2 & -1 & & & \mathbf{0} \\ -1 & 2 & -1 & & \\ & -1 & 2 & -1 & \\ & & \ddots & \ddots & \ddots \\ & & & -1 & 2 & -1 \\ \mathbf{0} & & & & -1 & 2 \end{pmatrix} \qquad \cdots\cdots(59)$$

$$(k, i = 1, 2, \ldots, N-1)$$

for the case of both ends fixed. The symbol **0** denotes that every matrix element in that part is zero.

Multiplying Eq. (58) by y_k and summing it up over all values of k, we have

$$(\Delta x)^2\lambda = \sum_{k=0}^{N}\sum_{i=0}^{N} b_{ki}y_k y_i \Big/ \sum_{k=0}^{N} y_k^2 . \qquad \cdots\cdots(60)$$

The lowest solution of Eq. (58) is the function y_k $(k=0, 1, 2, \ldots, N)$, which minimizes the right hand side of Eq. (60), and the corresponding λ is the lowest eigenvalue. This is true only if the quadratic form in the numerator of Eq. (60) is symmetric, i.e. if $b_{ki}=b_{ik}$.

Let us choose any function $\phi_k^{(0)}(k=0, 1, 2, \ldots, N)$ as a rough approximation to the solution y_k and then change each point in such a way as to lower λ at each step. The conditions for the vanishing of $\partial\lambda/\partial\phi_k$ suggest that λ will be lowered by replacing $\phi_k^{(0)}$ by

$$\phi_k^{(0)} = -\sum_i{}' b_{ki}\phi_i^{(0)} \Big/ \{b_{kk}-\lambda(\Delta x)^2\} . \qquad \cdots\cdots(61)$$

Where $\sum'$ denotes summation of all values of i except $i=k$. We shall now show that this change actually lowers λ if the lattice is not too coarse. Let $\Delta\phi_k = \phi_k^{(1)}-\phi_k^{(0)}$, then

$$\lambda^{(1)}-\lambda^{(0)} = \{\lambda^{(0)}(\Delta x)^2-b_{kk}\}\left[\frac{(\Delta\phi_k)^2}{\sum\phi_{(k)}^{(0)2}}-0\{(\Delta\phi_k)^3\}\right] \qquad \cdots\cdots(62)$$

is obtaind. If the number of lattice points is large, the second term may be neglected in comparison with the first one in the bracket [ ] of Eq. (62), and λ will be decreased by the change in ϕ_k if $\lambda^{(0)}(\Delta x)^2-b_{kk}$ is negative. But $\lambda^{(0)}(\Delta x)^2-b_{kk}$ may be certainly made negative by using a sufficiently fine lattice, since $\lambda^{(0)}$ is obtained in access to a certain value as Δx decreases.

Therefore, we may continuously decrease λ by using Eq. (61) as an improvement formula. As λ converges to the true lowest eigenvalue, the function must converge to the true lowest eigenstate.

(B) Eigenfrequency problem of the fourth order

Next, let us suppose the transverse vibration of uniform bar. The fundamental equation of the free vibration is given by

$$EI\frac{\partial^4 y}{\partial x^4}+\frac{\rho A}{g}\frac{\partial^2 y}{\partial t^2}=0 \quad (0\leqq x\leqq l), \qquad \cdots\cdots(63)$$

where EI, ρ and A are the flexural rigidity, unit weight and the cross sectional area of the bar respectively. By the suitable transformations of coordinate and time, we obtain

$$\frac{\partial^4 y}{\partial x^4}+\frac{\partial^2 y}{\partial t^2}=0 \quad (0\leqq x\leqq 1) \qquad \cdots\cdots(64)$$

When we consider only the simple harmonic oscillation,

$$\frac{d^4\bar{y}}{dx^4}-\lambda\bar{y}=0\,,\qquad \lambda=p^2 \qquad \cdots\cdots(65)$$

is obtained from Eq. (64). Replacing Eq. (65) by a set of the algebraic equations, we have

$$(\Delta x)^4\lambda y_k=\sum_{i=0}^{N}b_{ki}\,y_i \qquad (k=0,\,1,\,2,\,\ldots,\,N)\,. \qquad \cdots\cdots(66)$$

As the boundary conditions, let us consider one end fixed and the other free. Then

$$\left.\begin{aligned} &y_0=0,\quad y_1=y_{-1}\,,\\ &y_{N+1}-2y_N+y_{N-1}=0\,,\\ &y_{N+2}-3y_{N+1}+3y_N-y_{N-1}=0\,. \end{aligned}\right\} \qquad \cdots\cdots(67)$$

These are the algebraic boundary conditions.

In this case, the coefficient matrix takes the form:

$$(b_{ki})=\begin{pmatrix} 7 & -4 & 1 & & & & \mathbf{0}\\ -4 & 6 & -4 & 1 & & & \\ 1 & -4 & 6 & -4 & 1 & & \\ & 1 & -4 & 6 & -4 & 1 & \\ & \ddots & \ddots & \ddots & \ddots & \ddots & \ddots \\ & & 1 & -4 & 6 & -4 & 1\\ & & & 1 & -4 & 5 & -2\\ \mathbf{0} & & & & 1 & -2 & 1 \end{pmatrix} \qquad \cdots\cdots(68)$$

$(k,\,i=0,\,1,\,2,\,\ldots,\,N)$

which is obviously symmetric. Thus, the procedure may be developed similarly to that in (A).

(C) Further investigations to check the numerical solution

The rigorous solution of the free vibration of a string whose both ends are fixed was already solved as

$$y=A\sin\sqrt{\lambda}\,x\,,$$
$$\sqrt{\lambda}=n\pi\quad(n=1,2,\ldots)\,.$$

Therefore, the minimum eigenvalue is $\pi^2(\fallingdotseq 9.869604)$. On the other hand, the numerical results are given by Fig. 24 and Table 2. In spite of the rough trial

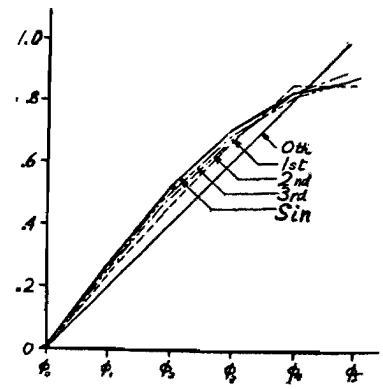

Fig. 24. Approximation for eigenfunction of case (A).

function, the results well agree with the theoretical ones. Next we investigate the case (B) whose eigenvalue is known as $\lambda \fallingdotseq (1.875104)^4 = 12.362$. The results of the numerical calculation in this case are seen in Table 3.

Table 2. Approximation for solution of case (A)

i \ $\phi^{(i)}\lambda^{(i)}$	$\phi_0^{(i)}$	$\phi_1^{(i)}$	$\phi_2^{(i)}$	$\phi_3^{(i)}$	$\phi_4^{(i)}$	$\phi_5^{(i)}$	$\lambda^{(i)}$
0	0	0.2	0.4	0.6	0.8	1.0	11.7647
1	0	.24386136	.45903317	.66406246	.84999997	.84999997	10.1607
2	0	.25483644	.48377971	.67454276	.82151409	.89549414	9.8818
3	0	.25868611	.49180914	.68018181	.80936909	.86421445	

$\lambda = \pi^2 \fallingdotseq 9.8696$, $\phi_i = \phi_{10-i} (i = 0, 1, 2, 3, 4)$

Table 3. Approximation for solution of case (B)

i \ ϕ, λ	ϕ_0	ϕ_1	ϕ_2	ϕ_3	ϕ_4	ϕ_5	ϕ_6	ϕ_7
1	0	.011	.032	.058	.090	.125	.164	.207
2	0	.009545	.031273	.058280	.089480	.125238	.164071	.206856
3	0	.005023	.030200	.058154	.089594	.125002	.164291	.206792
i \ ϕ, λ	ϕ_8	ϕ_9	ϕ_{10}	ϕ_{11}	ϕ_{12}	ϕ_{13}	ϕ_{14}	ϕ_{15}
1	0.253	.302	.353	.408	.465	.524	.586	.649
2	.252996	.301851	.353427	.407644	.465014	.524190	.585679	.649577
3	.252893	.301867	.353462	.407774	.464771	.524300	.585724	.649506
i \ ϕ, λ	ϕ_{16}	ϕ_{17}	ϕ_{18}	ϕ_{19}	ϕ_{20}	$\lambda^{(i)}$		
1	.716	.783	.852	.925	1.000	22.24		
2	.715231	.783465	.852467	.924200	.998000	14.16		
3	.715426	.783196	.852859	.923614	.995933	12.87		

$\lambda \fallingdotseq (1.875104)^4 \fallingdotseq 12.362$

In order to improve the approximation, we consider the higher difference in Eq. (55). The relations corresponding to Eq. (56) got by using the first three terms of Eq. (55) as the second order approximation and the first four terms as the third one, are given as follows :

$$\text{for 2nd approx.} \quad \left(\frac{d^2y}{dx^2}\right)_{x=xk} \simeq \frac{1}{12(\Delta x)^2}(y_{k-2} - 16y_{k+1} + 30y_k - 16y_{k+1} + y_{k+2})$$

$$\text{for 3rd approx.} \quad \left(\frac{d^2y}{dx^2}\right)_{x=xk} \simeq \frac{1}{180(\Delta x)^2}(-2y_{k-3} + 27y_{k-2} - 270y_{k-1} + 490y_k - 270y_{k+1} + 27y_{k+1} - 2y_{k+3}). \tag{69}$$

More improved results for Table 2 are shown in Table 4 using the relations (69).

Table 4. More developed approximation for eigenvalue of case (A)

Formula / No. of Approx	1st. approx.	2nd approx.	3rd. approx.
0	10.9091	9.9172	9.87035
1	10.2135	9.8764	9.882625
2	9.9385	9.8721	9.869643
3	9.8275	9.8693	9.869617
4	9.7952	9.8688	9.869591
5	9.7902	9.8686	9.869590
6	9.7890		
7	9.7888		
8	9.7887		

The Vibration Experiment of a Pile

As shown in Fig. 25, the test pile is oscillated horizontally by the oscillator (max. oscillating force 600 kg) mounted on the reinforced concrete hollow pile. The dimensions of the pile are as follows; Length of pile: 7.13 m, outer dia. of cross section of pile: 30 cm, inner dia. of cross section: 16 cm.

On the transverse vibration tests, the resonance curve of the pile and the reaction force of soil were studied.

The eigenfrequency for this case is evaluated by the numerical method described above. The fundamental equation is

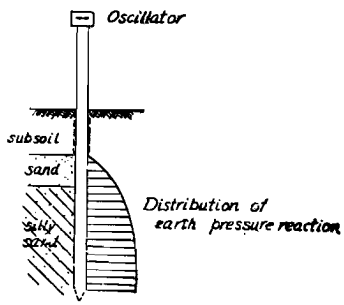

Fig. 25. Diagram illustrating vibration test of pile and assumed parabolic distribution of earth pressure reaction. For numerical calculation. Earth pressure reaction is 6 kg/cm³ at the lowest end.

$$EI\frac{\partial^4 y}{\partial x^4}+\frac{\rho A}{g}\cdot\frac{\partial^2 y}{\partial t^2}+2ayk(x)=0 \qquad \cdots\cdots(70)$$

and $k(x)$ is assumed as shown in Fig. 25, considering some experimental results. In the upper portion of the embedded pile, $k(x)$ is considered to vanish, because the ground surface has been loosened. Substituting $y=\bar{y}(x)e^{ipt}$ into Eq. (70), we have the difference equation:

$$\Lambda y_k=\sum_{i=1}^{N} b_{ki}\,y_i\,, \qquad \Lambda=\frac{\rho A p^2}{gEI}(\Delta x)^4 \qquad \cdots\cdots(71)$$

As the k-th diagonal element of the matrix (b_{ki}) is $6+\dfrac{2ak(x)}{EI}(\Delta x)^4$ and the

matrix is symmetric, a similar successive approximation to that used in the above method may be performed. The constants which are used in the numerical calculation are as follows: $2a = 0.3$ m, $A = 5.05 \times 10^{-2}\text{m}^2$, $\rho = 2.4\,t/\text{m}^3$, $E = 3.5 \times 10^6 t/\text{m}^2$, $I = 3.65 \times 10^{-4}\text{m}^4$ and $\Delta x = 0.3565$ m $(N = 20)$.

The result of the calculation is given by Table 5, and this value fairly agrees with the experimental value $T_{exp} = 0.13$ sec.[3], so that the distribution of the reaction force seems to be proper. But the question was left, because the vibration period is computed from the resonance curve by the forced vibration in this experiment.

Table 5. Comparison of numerical approximate eigenfrequency to experimental one.

No. of approx	A	$f_{\text{sec}^{-1}}$	T_{sec}
0th	19.9×0^{-4}	18.0	0.05_5
1st	$4.7_3 \times 10^{-4}$	8.7_8	0.11_3
2nd	$4.9_4 \times 10^{-4}$	8.6_9	0.11_5
experimental	—	7.7	0.13

4. The Measuring Instrument for Vibration

General Consideration of the Piezoelectric Crystal Vibration Pick-up

In research of the dynamic behavior of the foundation, the study of the measuring instrument must not be disregarded.

Recently in this branch, it is very remarkable that electronic means have come to be in frequent use in compliance with various objects. As the piezoelectric crystals used for a vibration transducer, there are quartz, ADP, rochelle salt and barium titanate ceramics[4]. Here we shall explain the accelerometer which was devised on trial, considering its stability, frequency characteristics and light weight due to barium titanate ceramics.

This may also be applied to the displacement vibrograph, the vibration earth pressure meter, etc., if they are modified in their design.

As one of the most important properties of the piezoelectric pick-up is that of the output circuit, the electric characteristics as an accelerometer are investigated, using following nomenclature:

M: loaded mass on the surface of the crystal
α: acceleration given to the mass M
δ: piezoelectric modulus
Q: electric charge excited in the crystal electrode by external force M
C_0: capacitance of the crystal
C_1: distributed capacitance of transmission lines
C_2: capacitance between cathode and grid of the first step vacuum-tube

R: equivalent resistance combined with grid leak and resistance between cathode and grid of the first step vacuum-tube
E: Output voltage of the crystal
i: electric current in resistance R.

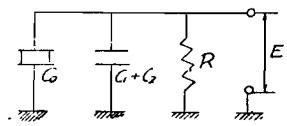

Fig. 26. Equivalent circuit of piezo-electric vibration pick-up and its output circuit.

Then, the equivalent circuit is shown in Fig. 26,[5] and the relations are obtained as follows:

$$E = iR = \frac{1}{C}\left(Q - \int i\,dt\right) \quad \cdots(72)$$

$$Q = \delta M \alpha \quad \cdots\cdots(73)$$

where $C = C_0 + C_1 + C_2$.

Removing i from eqs. (72) and (73), we have

$$\frac{dE}{dt} + \frac{E}{CR} = \frac{\delta M}{C}\cdot\frac{d\alpha}{dt}. \quad \cdots\cdots(74)$$

If CR is sufficiently large, in the left hand side the second term is negligibly small compared with the first term, so that

$$E \simeq \frac{\delta M}{C}\alpha. \quad \cdots\cdots(75)$$

This shows that the output voltage is proportional to the acceleration given to the mass. In the case of simple harmonic vibration, if α_m denotes the amplitude of the acceleration,

$$\frac{dE}{dt} + \frac{E}{CR} = \frac{\delta M}{C}\alpha_m p \cos pt \quad \cdots\cdots(76)$$

is derived from Eq. (74), where p is the circular frequency of the acceleration. The solution of Eq. (76) is easily given by

$$\left.\begin{aligned} E &= \Gamma e^{-\frac{t}{CR}} + \frac{\delta M \alpha_m}{C}\cdot\frac{1}{\sqrt{1+\frac{1}{(PCR)^2}}}\sin(pt+\varepsilon), \\ \varepsilon &= \tan^{-1}\frac{1}{PCR}, \end{aligned}\right\} \quad \cdots\cdots(77)$$

where Γ is a constant which is determined by an initial condition and ε denotes the phase difference. On the stationary state, it is sufficient to consider only the second term, as the first term vanishes. The term $1/\sqrt{1+1/(PCR)^2}$ in the second term is the coefficient of sensitivity which represents the frequency characteristics. If $pCR \gg 1$ in Eq. (77), it is obvious that $\varepsilon \simeq 0$ and $E \simeq \frac{\delta M}{C}\alpha$ which are most convenient conditions for accelerometer.

Mechanical Characteristics and Structure of the Piezoelectric Crystal Accelerometer

For the sake of brevity, suppose a simple vibration system which consists of a mass M and a spring s as shown in Fig. 27. In order to make the motion of the mass proportional to the acceleration of the casing of this system, it is necessary that the eigenfrequency f_0 $(=1/2\pi\sqrt{M/s})$ of the system should be adopted to be far larger than the frequency of the external force. And if a piezoelectric crystal is used as a spring of the system satisfying the above frequency condition, a favourable accelerometer will be obtained.

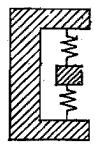

Fig. 27. Vibration system with mass and spring

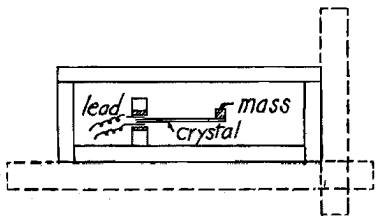

Fig. 28. Structure of piezoelectric accelerometer.

For our trial accelerometer, its eigenfrequency is taken as 500 c.p.s., which is far larger than the actual frequency 5~50 c.p.s. expected on the measurement in soils. A barium titanate ceramic bar of 0.55 mm ×2.2 mm ×18 mm is used as a cantilever, one end of which is fixed and the other attached to a mass and kept free (see Fig. 28). The attached mass is 1 gr in weight. The total weight of the pick-up is about 100 gr and can be adjusted to have the same unit weight with soils.

The Amplifier and the Results of Calibration

As described above, the condition $PCR \gg 1$ should be satisfied in the output circuit of the accelerometer. It is, however, trivial to insert higher resistors than the grid resistance of a vacuum-tube, which is generally 10^8 ~10^9 ohm. On the other hand, the capacitance should be restrained to be not so large from the view of sensitivity, but the trial amplifier is inserted with a certain capacitance. As the result of this, the sensitivity is lowered to some extent, but there occurs a merit of decreasing effect of leak in the transmission lines. If it is assumed that the

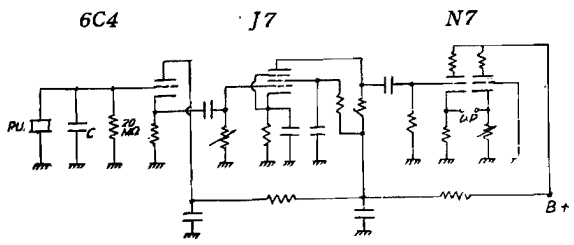

Fig. 29. Network of trial amplifier.

minimum freqency is 5 c. p. s., $R = 20\,M\Omega$ and $C = 0.02\,\mu F$., then the error of the amplitude of acceleration is calculated as nearly 3% and the angle of the phase difference 30′. The amplifier circuit thus made is shown in Fig. 29, and it is desirable to use a galvanometer of about 100 c. p. s.

The calibration test of the above accelerometer and the amplifier has been made by using the electro-dynamic testing vibrograph, and the result is shown in Fig. 30. This figure represents the combined characteristics of the accelerometer and the amplifier obtained, excluding that of the galvanometer of 30 c. p. s. which was used in our test for an unavoidable reason. From the figure, the frequency characteristics are perfectly constant. If a galvanometer with eigenfrequency of more than 100 c. p. s. is used, the synthetic characteristics would be also flat.

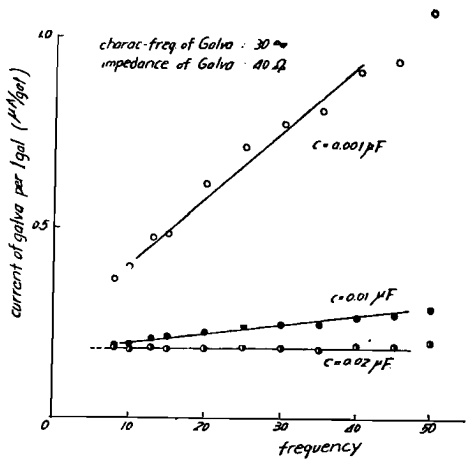

Fig. 30. Frequency characteristics of trial accelerometer and amplifier.

This accelerometer is designed for both a vertical and horizontal vibrograph. With this accelerometer, the vibration displacement can be obtained by integrating the record of acceleration by means of a suitable integraph such as the analogue computor.

References

1) Den Hartog, Mechanical vibrations, 2nd. ed., 403, (1940).
2) G. E. Kimball and G. H. Shortley, The numerical solution of Schrödinger's equation, Phys. Rev., **45**, 815, (1934).
3) H. Gotō and Y. Maeda, On the reaction force of foundation ground, read at the 10th meeting of Jap. Soc. Civ. Eng., (May, 1954).
4) B. Baumzweiger, Application of piezoelectric vibration pick-up to measurement of acc., velo. and dispt., Jour. Acous. Soc. America, **11**, 303, (1953).
T. Tanaka, Barium titanate ceramics as electro-mechanical transducer, Jour. Jap. Soc. Test. Mat., **2**, 404, (1953).
5) T. Hagihara, Vibration measurement, 4th. ed., 265, (1951).